

Carbon arc plasma: characterization and synthesis of nanosized SiC

O Łąbedź¹, A Huczko¹, J Gawraczyński¹, H Lange¹, C Czosnek² and J F Janik²

¹Department of Chemistry, Warsaw University, 02-093 Warsaw, Poland

²AGH University of Science and Technology, 30-059 Cracow, Poland

E-mail: olabedz@gmail.com; ahuczko@chem.uw.edu.pl

Abstract. Silicon carbide SiC is an important ceramic material with many applications. The nanomaterials can possess novel electronic and mechanical properties. Thus, we attempted to produce SiC nanopowder via a fast, one-step direct plasma synthesis. Two experimental systems were tested regarding the efficiency of SiC formation (for comparison): (i) arc plasma and (ii) high-temperature aerosol route. The products were characterized by wet chemical analysis, X-ray diffraction (XRD) and scanning electron microscopy (SEM). Almost total plasma conversion of starting Si-bearing reactants (Si, SiO and SiO₂) was achieved with SiC nanopowder (well below 100 nm) as a main product. From the emission spectroscopy measurements the arc plasma temperatures were evaluated to be within 3500-6000 K.

1. Introduction

Silicon carbide (SiC) and its composites have found wide applications because of its high Young's modulus and hardness, excellent oxidation and corrosion resistance, high strength at elevated temperatures, good thermal shock durability and electronic characteristics [1]. In addition, nanocrystalline SiC attracts considerable attention because of the wide band gap and quantum size effects [2]. Thus, the SiC nano-crystallites can be used to fabricate electronic devices which are durable at high temperature, strong radiation and fierce erosion. Several methods to produce nano-SiC have been proposed, such as combustion synthesis [3], chemical vapour deposition (CVD) [4], ion implantation [5], heat synthesis [6] and electrochemical etching [7]. Those routes usually suffer, however, from low productivity and long reaction duration. In this paper, we compare two different novel approaches to prepare SiC nanocrystallites. Not only we study the overall process efficiency, but also the oxygen presence in the reaction zone has been tested since in our earlier work we found [8] its profound influence on the formation of β -SiC nanowires synthesized via a combustion route (SHS). The on-line emission spectroscopy was carried out for a carbon plasma diagnostics, too.

2. Experimental

The plasma runs were carried out in the experimental system shown in figure 1 and described in details elsewhere [9]. The arc gap and its position against the optical axis was controlled automatically. The system allowed for holding the electrode gap between 1 and 2 mm for at least 5 minutes of arc operation, during which the radiation emission was measured. The home-made sintered anodes were prepared using the powdered mixtures of carbon black with either Si elemental, SiO or with SiO₂. Arc sublimation/reduction of reactants were performed under He-O₂ low pressure (300 hPa) at the arc current within 10-50 A. The gas-phase condensed products were collected for the



following analyses. For comparison, an attempt was also made to obtain SiC nanopowder via a 2-step high-temperature pyrolysis of a hexamethyldisiloxane and polydimethylsiloxane in the system and applying the procedure outlined elsewhere [10]. The reaction products were further examined using SEM, XRD and wet chemistry techniques. Carbon arc set-up with spectroscopic arrangement is shown in figure 1. The details of the experimental and computational protocols of carbon arc plasma diagnostics were presented earlier [11].

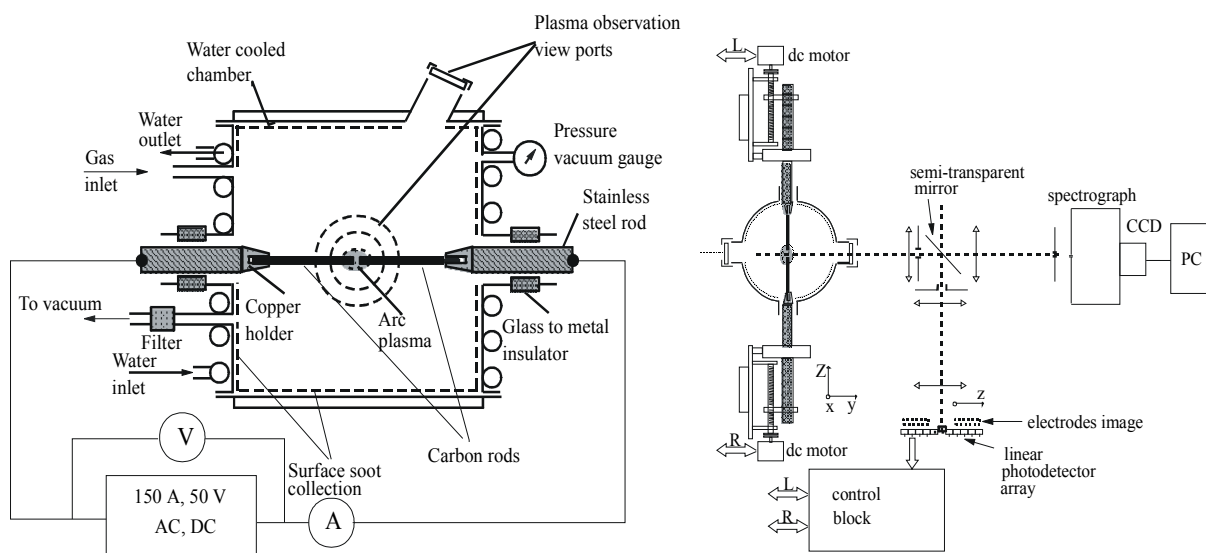


Figure1. Carbon arc set-up with spectroscopic arrangements.

3. Results and discussion

3.1. Plasma spectroscopy

The aim of the carbon arc plasma diagnostics was to determine the temperature distribution in the coalescent zone, i.e. in the vicinity of the arc gap. For the diagnostics of the plasma containing carbon gas the most suitable is the Swan band system ($d^3\Pi_g - a^3\Pi_u$), particularly the mostly exploited 0-0 band at 516.5 nm, emitted by C_2 radicals. The same molecular spectrum can also be used when the gas phase contains additionally silicone vapor and oxygen. Indeed, in such a case C_2 bands are the major constituent of the plasma radiation in the optical range. The carbon vapor pressure in the arc under conditions favoring formation of nanocarbons, e.g., fullerenes, CNTs and silicon carbides can be quite high. Therefore, depending the electrode erosion rate, this resonant band, and mainly its 0-0 head, can be disturbed by the self-absorption phenomenon. Thus, it has to be taken into account when gas temperature is determined from the rotational structure of the band. Moreover, if significant, this effect can be used for the simultaneous temperature and C_2 radical concentration determination. We applied here a method based on the effect of self-absorption within the band, which has been routinely used by us for years [11]. Generally, the method is based on the calculation of the spectrum assuming different temperatures and optical densities associated with the transition $a^3\Pi_u, v''=0 - d^3\Pi_g, v'=0$. Next, the calculated spectra are fitted into experimental ones. The best fit is equivalent to the particular values of $C_2(d^3\Pi_g, v'=0)$ column density (product of density and plasma column length), as well as average temperature along a plasma column. The details of the calculation procedure and its practical application have been described elsewhere [12]. When calculating spectra, a Voigt profile was taken into account. In contrast to pure carbon arc under similar graphite electrode erosion rate, the presence of Si and O in arc plasmas lowers significantly C_2 concentration resulting in much lower optical density of C_2 radical radiation. Two examples of C_2 (0-0) Swan spectra for low (10 A) and high (50 A)

arc currents, taken at plasma coordinate 8 mm from the arc centre, are shown in figure 2, left and right respectively. Indeed, in the first case the C_2 column density was too low for any self-absorption detection. At the higher arc current the self-absorption was higher, but still on the verge of its detection.

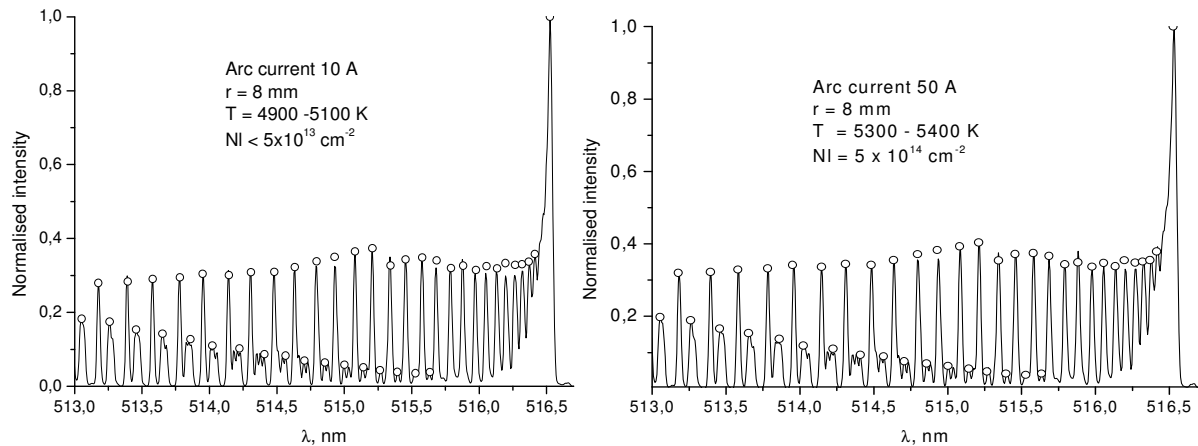


Figure 2. Examples of experimental spectra C_2 ($d\ ^3\Pi_g - a\ ^3\Pi_u$, 0-0). Markers are characteristic points taken from simulated spectra.

On the basis of the temperature and $C_2(d\ ^3\Pi_g, v'=0)$ density values one could estimate the global carbon vapor pressure assuming thermodynamic equilibrium. The results point to pressure values about 1 and 7 kPa, respectively, for the arc conditions in figure 2.

Radial temperature distributions are shown in figure 3. Different S-bearing reactants (Si, SiO, SiO₂) used to fabricate the anodes do not alter these results.

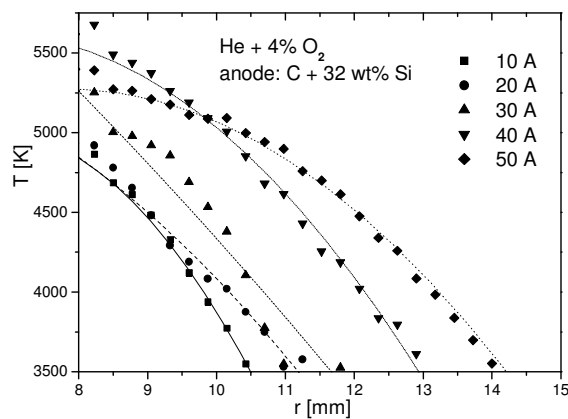


Figure 3. Radial temperature distributions in the arc vicinity.

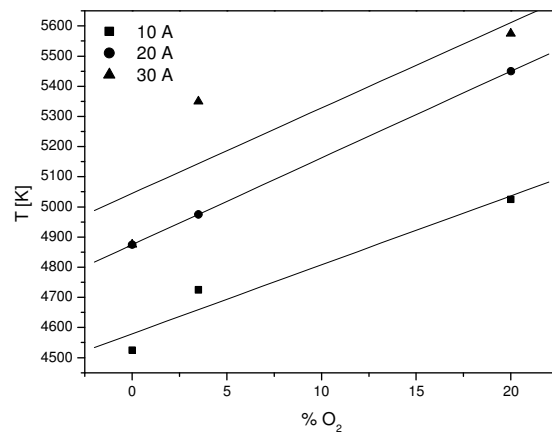


Figure 4. Influence of O_2 on temperature, $r = 8$ mm.

The only parameters influencing the temperature distributions are the arc current (figure 3), which causes mainly plasma zone broadening, and also O_2 content in He. With the increasing O_2 partial pressure the temperature increases, this due to possible exothermal effect of partial carbon oxidation, accompanying the SiC formation. Figure 4 confirms this observation.

3.2. Carbon arc plasma processing

From the presented SEM images (figure 5) a nanosized dimension of collected powders is evident. Spherical objects well below 100 nm dominate (soot and SiC nanoparticles). Some well-crystallized SiC 3-D microcrystallites can be also spotted. Some images reveal a web-like morphology of products. The study is under way (via controlled oxidation) to verify whether the obtained 1-D nanostructures are either carbon nanotubes or β -SiC nanowires.

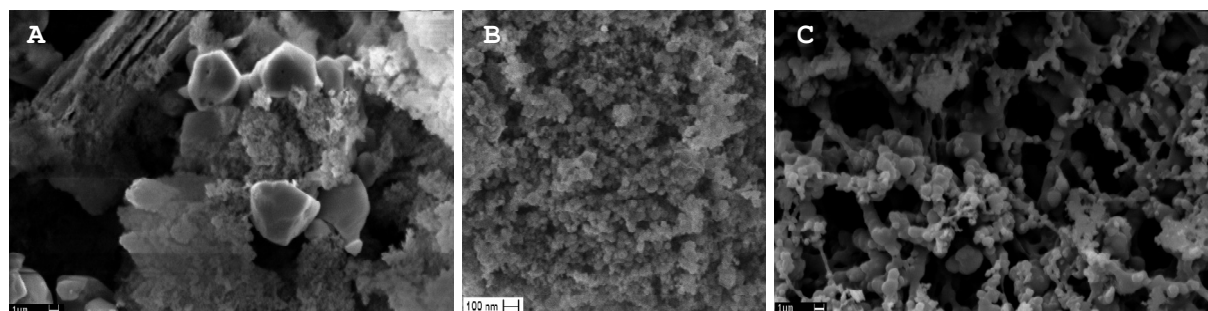


Figure 5. SEM images of arc plasma products (A – SiO₂ in He, B - Si in He + 20% O₂ and C – SiO₂ in He with 20% O₂).

Figure 6 shows XRD spectra of produced powders. Relatively low intensity of characteristic patterns (almost entirely assigned to β -SiC) proves low crystallization and nano-dimensionality of a product.

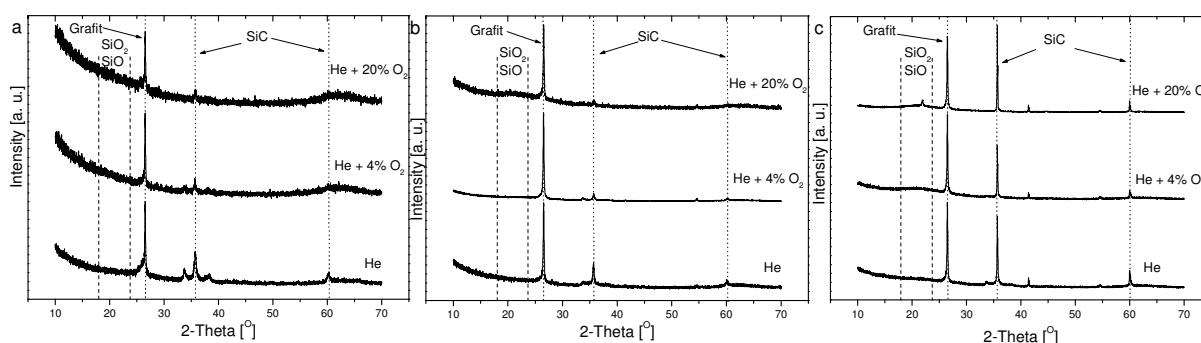


Figure 6. XRD spectra of products obtained from electrodes containing a – Si, b – SiO and c - SiO₂.

The products resulting from carbon arc-sublimated Si-containing graphite anodes (A: 68 wt% C – 32 wt% Si; B: 58 wt% C – 42 wt% SiO and C: 49 wt% C – 51 wt% SiO₂) in He-O₂ atmosphere were chemically analysed (via reaction with boiling 30 wt% KOH) for the determination of free Si. The results are shown in table 1. Very low content of un-reacted Si in the products proves high degree of reduction/conversion of the starting Si-bearing reactant into SiC.

Table 1. Results of chemical analysis of products.

Atmosphere (300 hPa)	Starting electrode A	Starting electrode B	Starting electrode C
He pure	2,8 wt% Si	0 wt% SiO	2,9 wt% Si
He 96% - O ₂ 4%	2,1 wt% Si	0 wt% SiO	1,8 wt% Si
He 80% - O ₂ 20%	1,6 wt% Si	~ 25 wt% SiO	0 wt% Si

3.3. Aerosol-route pyrolysis

An attempt was made to use various Si-bearing organic precursors to obtain nano-SiC powder of relatively large specific surface (determined by BET) by a pyrolytic route. Figure 7 shows SEM images of nanoproducts obtained using (A) DC Ar plasma, for comparison, and (B) aerosol routes. The products from the aerosol route have a spherical, homogeneous morphology.

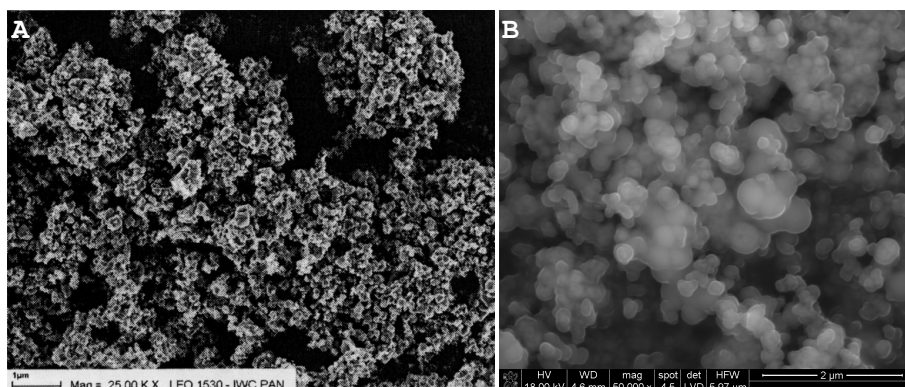


Figure 7. SEM images of SiC products resulting from DC plasma, flow system (1A) and aerosol pyrolysis (1B).

XRD spectra of products are shown in figure 8 and confirm the presence of regular β -SiC phase. Plasma product is a very fine, semi-amorphous SiC powder, while SiC from aerosol route is much better crystallized. FT-IR spectra for plasma (A) and aerosol-route (B) products have (figure 9) a wide absorption at ca 820 cm^{-1} (Si-C binding oscillations) while 1046 cm^{-1} absorption can be assigned to Si-O oscillation. BET measurements also showed relatively high specific surface (up to $50\text{ m}^2/\text{g}$) for aerosol route-synthesized nano-SiC.

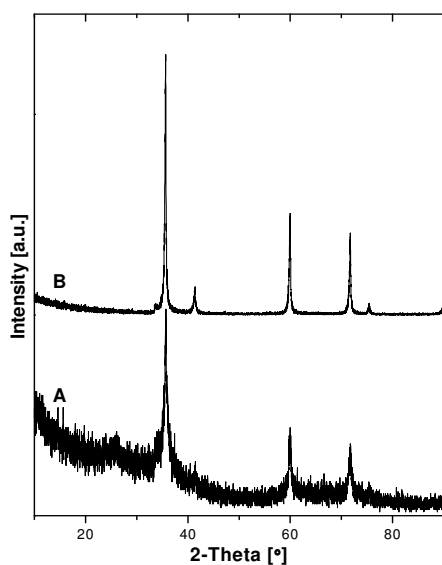


Figure 8. XRD spectra of products resulting from plasma and 2-stage aerosol route.

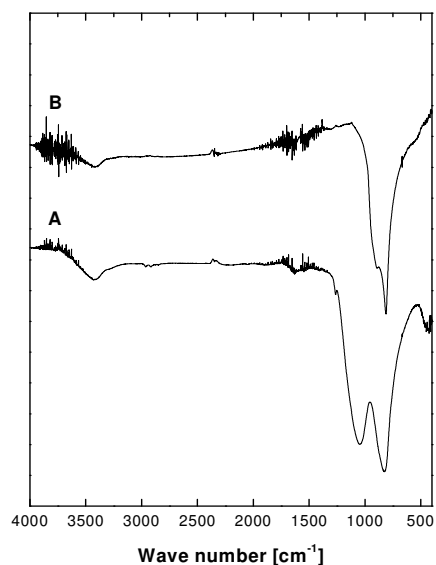


Figure 9. FT-IR absorption of products resulting from plasma and 2-stage aerosol route.

4. Conclusions

Si-bearing reactants efficiently yield SiC nanopowder, regardless of their nature and the experimental system used. The total conversion does not rely directly either on oxygen content in the starting compounds or an oxygen content in the arcing environment. It proves that under plasma conditions silicon carbonization towards SiC is faster comparing to simple oxidation. We envisage the silicon mass transfer via gaseous SiO which is a relatively stable molecule in the gas phase. Thus, the oxygen-containing atmosphere obviously will favour the efficient formation of SiO. In fact, SiO involvement and Si catalytic role in the process of SiC growth have been already suggested [13] Surprisingly, the plasma temperature (within 3500-6000 K) does not seem to depend on process operating variables. Comparing to the plasma processing, a pyrolytic aerosol route yields more homogeneous and better crystallized nano-SiC, but the productivity is lower and the total reaction time is much longer.

5. References

- [1] Liu G, Yang K, Li J, Yang K, Du J and Hou X, 2008 *J. Phys. Chem. C* **112** 6285
- [2] Du K, Yang H, Wei R, Li M, Yu Q, Fu W, Yang N, Zhu H and Zeng Y 2008 *Mat. Res. Bull.* **43** 120
- [3] Huczko A, Lange H, Chojecki G, Cudziło S, Zhu Y Q, Kroto H W and Walton D R M 2003 *J. Phys. Chem. B* **107** 2519
- [4] Mo Y H, Shajahan M, Lee K S, Kim K C, Cha O H, Suh E K and Nahm K S 2002 *Diamond Relat. Mater.* **11** 1701
- [5] Liao L S, Bao X M, Yang Z F and Min N B 1995 *Appl. Phys. Lett.* **66** 2382
- [6] Shen G Z, Chen D, Tang KB, Qian Y T and Zhang S Y 2003 *Chem. Phys. Lett.* **375** 177
- [7] Petrova-Koch V, Sreseli O, Polisski G, Kovalev D, Muschik T and Koch F 1995 *Thin Solid Films* **255** 107
- [8] Huczko A, Osica M, Rutkowska A, Bystrzejewski M, Lange H and Cudziło S 2007 *J. of Physics: Cond. Matt.* **19** 395022
- [9] Lange H, Baranowski P, Byszewski P and Huczko A, 1997 *Rev. Sci. Instrum.* **68** 3723
- [10] Czosnek C and Janik J F, 2008 *J. Nanosci. and Nanotechn.* **8** 907
- [11] Lange H and Huczko A, 2001 *Diamonds and Frontier Carbon Technology* **11** 399
- [12] Lange H, Saidane K, Razafinimanana M and Gleizes A, 1999 *J. Phys. D: Appl. Phys.* **32** 1924
- [13] Zhang J, Wang Q, Wang F, Chen X, Lei W, Cui Q and Zou G, 2009 *J. Phys. D: Appl. Phys.* **42** 035108

6. Acknowledgments

This research was co-financed by the European Regional Development Fund within the Innovative Economy Operational Program 2007-2013 under the project "Development of technology for a new generation of the hydrogen and hydrogen compounds sensor for applications in above normative conditions" (grant No. UDA-POIG.01.03.01-14-071/08-03). CC and JFJ acknowledge a financial support from AGH University of Science and Technology under the grant No. 11.11.210.120.